Supplorting Information

Full-spectrum responsive WO_{3-x}@HA nanotheranostics for NIR-II photoacoustic imaging-guided PTT/PDT/CDT synergistic therapy

Yanwen Ding, Rongtao Huang, Liuruiqi Luo, Wenwei Guo, Chengyuan Zhu, Xing-Can Shen*

State Key Laboratory for Chemistry and Molecular Engineering of Medicinal Resources, School of Chemistry and Pharmaceutical Science, Guangxi Normal University, Guilin, 541004, P. R. China.

*Corresponding Author: xcshen@mailbox.gxnu.edu.cn.

Materials and methods

Materials

Tungsten trioxide (< 100 nm) was purchased from Macklin (Shanghai, China). Sodium borohydride was purchased from Innochem (Beijing, China). Nitrotetrazolium blue chloride (NBT), terephthalic acid (TA), methylene blue (MB), disodium terephthalate, 5,5'-dithio bis-(2-nitrobenzoic acid) (DTNB), glutathione (reduced) and 5,5-dimethyl-1-pyrroline N-oxide (DMPO) were purchased from Aladdin Bio-Chem Technology Co., Ltd (Shanghai, China). Tetraacetoxymethyl ester (Calcein-AM) and 3,8-diamino-5-[3-(diethylmethylammonio) propyl]-6-phenylphenanthridinium diiodide (PI) were obtained from Sigma-Aldrich (Boston, MA, USA).

Synthesis of WO_{3-x}

As indicated in Scheme 1, WO_{3-x} NPs were synthesized using a simple one-step reaction using the megathermal reduction reaction of WO_3 nanopowder. 0.96 g of WO_3 nanopowder was weighed and mixed evenly with 0.3 g $NaBH_4$ and then placed in a tube furnace and heated to 430 °C in an argon atmosphere, this was maintained for 2 h. After the annealing treatment, the sample was washed with water several times to remove the excess $NaBH_4$. Then, the sample was dried in a vacuum drying oven to obtain the black WO_{3-x} containing oxygen vacancies.

Synthesis of WO_{3-x}@HA

Hyaluronic acid (1 g) was weighed and dissolved in 100 mL deionized water, then 50 mg of WO_{3-x} was added, this was stirred at 90 °C for 1 h, before the solution was transferred into a hydrothermal reactor, and reacted at 90 °C for 8 h. The solution was then washed with deionized water and dried to obtain WO_{3-x}@HA.

Characterization

Field emission transmission electron microscopy (TEM) images were recorded using a Thermo Fisher Scientific Talos F200S at 200 kV. X-ray photoelectron spectroscopy (XPS) was performed using an ESCALAB 250Xi. The X-ray diffraction (XRD) spectra were acquired using a Rigaku-D/MAX 2500v/pc. Electron paramagnetic resonance spectrometry (EPR) spectra were acquired using a Bruker A300. The UV-vis-NIR spectra were collected from 200 to 1300 nm using a Shimadzu spectrometer (UV-2600). The FTIR spectra were recorded from 400 to 4000 cm^{-1} using a Perkin-Elmer LS-55 FTIR spectrometer at room temperature. ICP-MS analysis results were acquired using a FLexar-NexION300X (Perkin Elmer).

Photothermal effect of WO_{3-x}@HA *in vitro*

800 μL of water and WO_{3-x}@HA (250 μg/mL) were added into EP tubes separately and irradiated using a continuous 1064 nm laser with a 1.0 W/cm^2 laser power intensity for 10 min to evaluate the photothermal efficiency. Infrared thermograms and temperatures were recorded using an infrared thermal camera (MAG30). The lasers (1.0 W/cm^2) were turned off after WO_{3-x}@HA (250 μg/mL) had been irradiated for 10 min, and the laser was turned on again after the temperature had dropped to room temperature. The temperature-time stability curve was drawn after 5 cycles of operation to evaluate the photothermal stability.

ROS generation of WO_{3-x}@HA *in vitro*

The generation of $\cdot O_2^-$ was measured using a commercial reagent, NBT. H_2O and WO_{3-x}@HA (250 μg/mL) were mixed with 10 μM of NBT, respectively. After irradiation with a 1064 nm laser (1.0 W/cm^2) for 10 min the absorption curves of NBT were monitored using UV-vis-NIR spectroscopy. The ·OH production ability of WO_{3-x}@HA was detected by using TA as a fluorescent substrate. H_2O and WO_{3-x}@HA (250 μg/mL) were mixed with 10 μM of TA, irradiated with a 1064 nm laser (1.0 W/cm^2) for 10 min, and then 100 μM H_2O_2 was added to WO_{3-x}@HA (250 μg/mL) and this was reacted for 10 min, finally, the fluorescence spectrum of this solution was detected using a fluorescence spectrometer at an excitation wavelength of 312 nm and emission wavelength of 425 nm.

Depletion of GSH *in vitro*

WO_{3-x}@HA bicarbonate buffer solution (250 μg/mL) was mixed with 20 μL of GSH (0.1 M). These tubes were incubated for different periods of times at 37 and 50°C, respectively. Then, the solution was centrifuged at 14000 rpm for 10 min. 200 μL of Ellman's reagent (5,5'-dithiobis (2-nitrobenzoic acid), DTNB) (0.5×10^{-3} M) was added into each of the collected supernatants, then the absorbance of the mixture was recorded at 410 nm. 7702 (human liver normal cell line) cells, 4T1 (mouse breast cancer cell line) cells and HeLa (human cervical cancer cell line) cells were used to detect the depletion of cellular GSH. After incubation with WO_{3-x}@HA for different times, the cells were washed three times with PBS solution. The collected cells were broken using an ultrasonic cell disruptor and centrifuged at 2500 rpm for 5 min, DTNB (0.5×10^{-3} M) was added to the supernatant solution, and the absorbance of the solution was recorded at 410 nm using a UV-vis spectrometer.

Intracellular ROS detection

7702 cells, 4T1 cells and HeLa cells were cultured with WO_{3-x}@HA for 6 h at 37 °C, respectively. Subsequently DCFH-DA was added to these cells and they were incubated for 30 min in the incubator, followed by exposure to laser irradiation (1.0 W/cm^2) or incubation in the dark for 10 min. Images of the intracellular activated DCFH fluorescence in these cells were recorded using a confocal microscope.

Cell cytotoxicity of WO_{3-x}@HA

The CCK-8 assay was used to determine the cell cytotoxicity of WO_{3-x}@HA in 7702 and 4T1 cells. 7702, 4T1 and HeLa cells were seeded into 96 well plates and incubated for 24 h in 180 mL culture medium, respectively. Then, different concentrations of WO_{3-x}@HA were added to the plates and they were incubated for 48 h. Next, 10 μL of CCK-8 solution was added to the plates and they were incubated for 30 min. Finally, a microplate reader was used to monitor the absorbance at 450 nm. In order to analyse the effect of WO_{3-x}@HA for in vitro treatment, the viability of the 4T1 cells was investigated after different treatments: (1) PDT, WO_{3-x}@HA was added to the cell culture medium and incubated for 8 h, the cell culture plate was placed on the surface of ice and each hole was irradiated for 5 min with a 1064 nm laser; (2) PTT, WO_{3-x}@HA was added to the cell culture medium, ascorbic acid was added to the cell culture medium after 4 h, and each hole was irradiated for 5 min with a 1064 nm laser after 4 h; (3) CDT, 100 μM H_2O_2 was added to the cell culture plate, the culture medium was changed after 4 h and WO_{3-x}@HA was added and incubated for 8 h; (4) PTT + PDT + CDT, 100 μM H_2O_2 was added to the cell culture medium, the culture medium was changed after 4 h, WO_{3-x}@HA was added and it was incubated for 8 h, each hole was irradiated with a 1064nm laser for 5 min. Then, CCK-8 analysis was performed for all cell plates to calculate the cell survival rate with different treatments.

Cell targeting experiment

To investigate the capability of WO_{3-x}@HA to target tumour cells, 7702, 4T1 and HeLa cells were inoculated into 6 well plates and incubated for 24 h. These cells were then incubated with or without HA (5 mg/mL) for 2 h, the cells were washed thrice with PBS then WO_{3-x}@HA (250μg /mL) was added and incubated for different periods of time. Then, these cells were washed thrice with PBS to remove the WO_{3-x}@HA that was not taken up by the cells. The cells were collected and underwent nitrification, before the W contents were quantitatively analysed using ICP-MS.

Photoacoustic imaging *in vivo*

The Balb/c female mice (6 weeks old) in this experiment were purchased from Hunan SJA Laboratory Animal Co., Ltd., (Hunan, China). WO_{3-x}@HA (100 μL, 500 μg/mL) was injected into 4T1 tumour-bearing mice via the caudal veins. Then, the PA images were recorded using a MSOT imaging system at 0, 4, 8, 12, 24, 36 and 48 h after injection, respectively (iThera Medical GmbH, Germany, $\lambda ex = 1064$ nm).

Photothermal imaging *in vivo*

The 4T1 tumour-bearing mice were randomly divided and assigned to two groups (five mice per group). Each mouse had a tumour of approximately the same weight (16 g) and a volume of 60-100 mm^3. Saline (100 μL) and WO_{3-x}@HA (100 μL, 500 μg/mL) were injected into these mice via the caudal veins, respectively. The tumour site was irradiated with a 1064 nm laser for 5 min while the thermograms and temperatures were recorded in the tumour region of the mice using an infrared thermal camera.

Synergistic effect of PTT/PDT/CDT *in vivo*

For construction of the tumour model, 50 μL of 1640 culture medium containing 4T1 cells (2×10^6) was inoculated subcutaneously into the right rear flank of each mouse. When the average tumour volume reached about 70 mm^3, the mice were randomly divided into four groups, each containing five mice, they then received different materials via injection and different treatments. Group 1: saline (100 μL); Group 2: WO_{3-x}@HA (100 μL, 500 μg/mL); Group 3: saline (100 μL) + 1064 nm laser; Group 4: WO_{3-x}@HA (100 μL, 500 μg/mL) + 1064 nm laser. After 12 h of injection, the tumours on the mice in Groups 3 and 4 were exposed to a 1064 nm laser (1.0 W/cm^2) for 10 min, and temperatures were recorded using an infrared thermal camera. The tumour size and body weight of the mice in each group were detected and recorded every day. The tumour volume was calculated according to the formula: V = length × $width^2$ / 2.

***In vivo* biocompatibility assay of WO_{3-x}@HA**

The mice in each group were euthanized by cervical dislocation after 14 d of treatment. The main organs from the mice (heart, liver, spleen, lungs, kidneys) and tumour tissues were collected in the experimental and control groups, soaked in 10% formalin, embedded, sectioned and stained using haematoxylin and eosin (H&E), optical microscopy images were obtained for histological analysis.

***In vivo* biodistribution assay of WO_{3-x}@HA**

The mice were euthanized after repeated injection of the same dosage of WO_{3-x}@HA (100 μL, 500 μg/mL) at 3 h, 6 h, 12 h, 24 h, 7 d, and 14 d, respectively, and their primary organs (heart, liver, spleen, lungs, kidneys) and tumour tissues were collected. After nitrification of these organs and tumour tissues, the content of W was quantitatively analysed using ICP-MS.

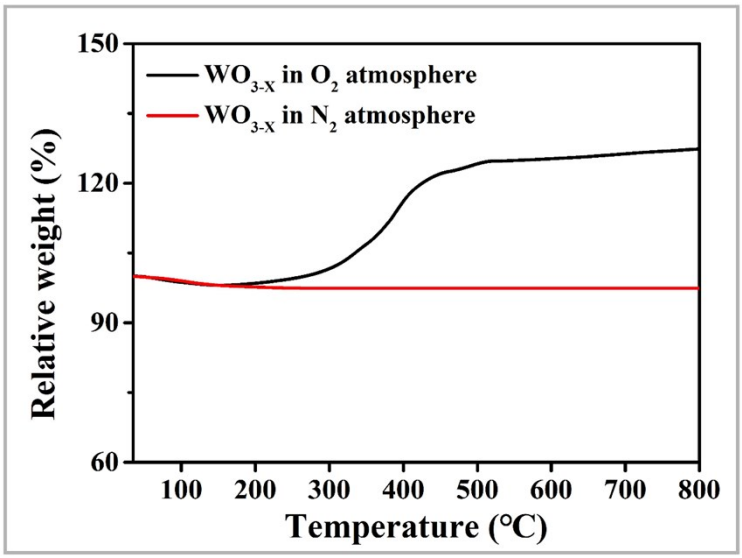

Fig. S1 TGA profiles of the WO_{3-x} at the heating rate of 10 °C/min in oxygen and nitrogen atmosphere.

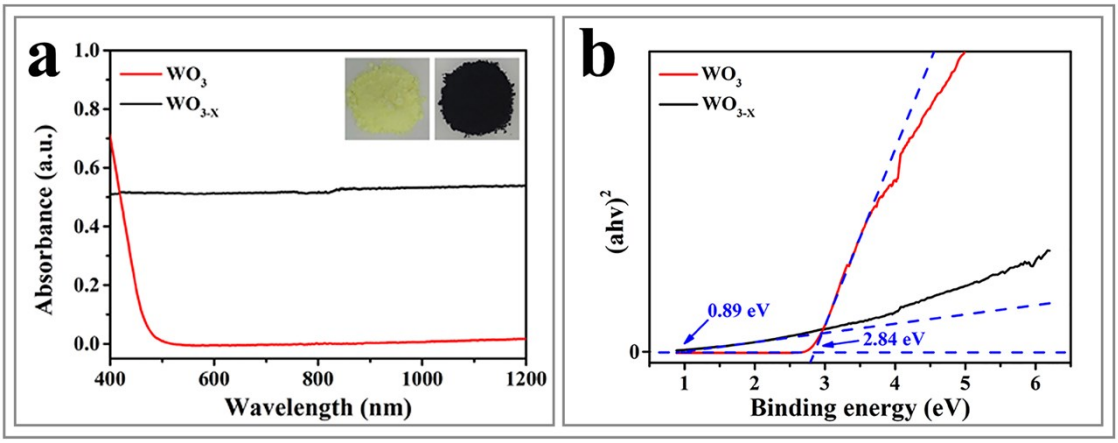

Fig. S2 (a) UV-vis-NIR diffuse reflectance spectra of WO_3 and WO_{3-x} (inset are the WO_3 and WO_{3-x} images). (b) Tauc plots obtained from the UV-vis-NIR spectra of WO_3 and WO_{3-x}.

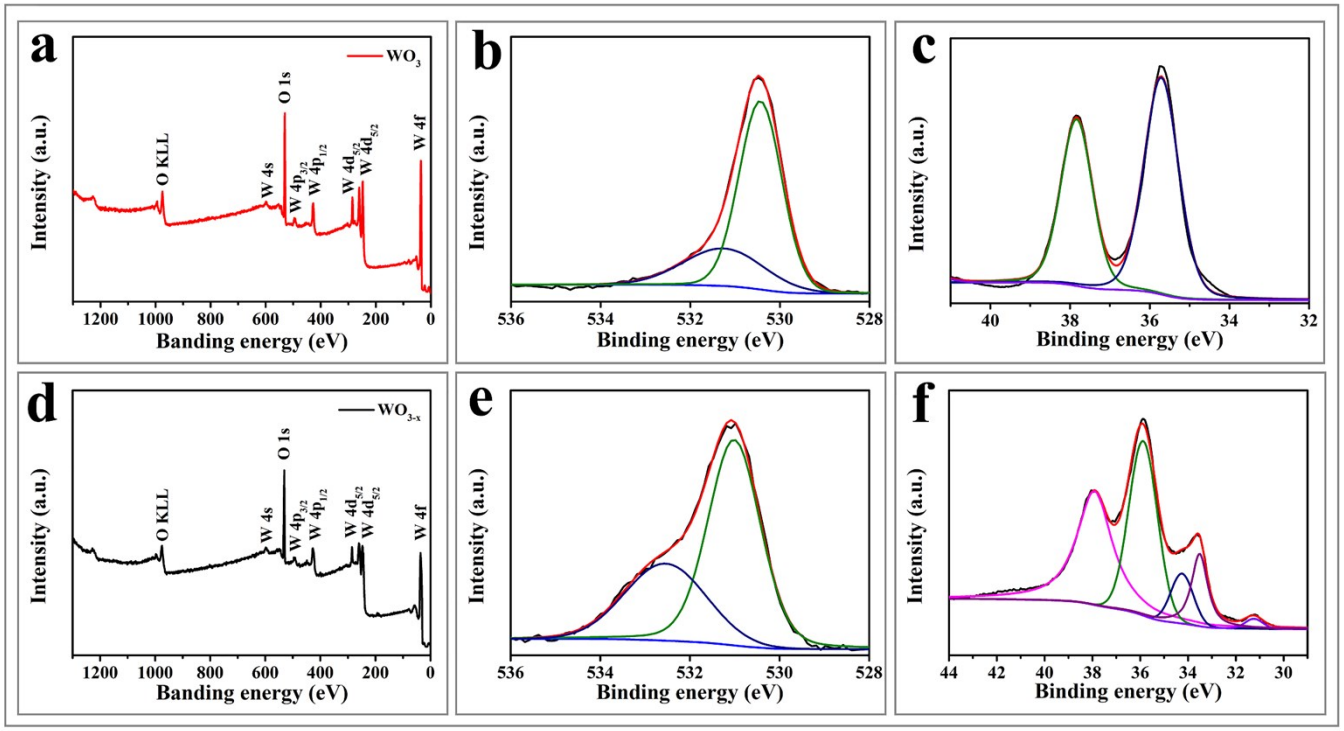

Fig. S3 The survey of full spectrum (a), O 1s (b), W 4f (c) of core level spectrum of WO_3. The survey of full spectrum (d), O 1s (e), W 4f (f) of core level spectrum of WO_{3-x}.

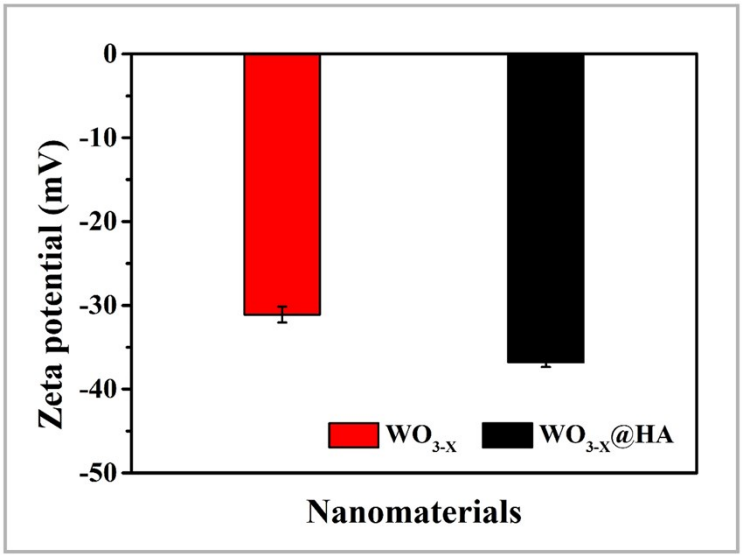

Fig. S4 Zeta potential of WO_{3-x} and WO_{3-x}@HA.

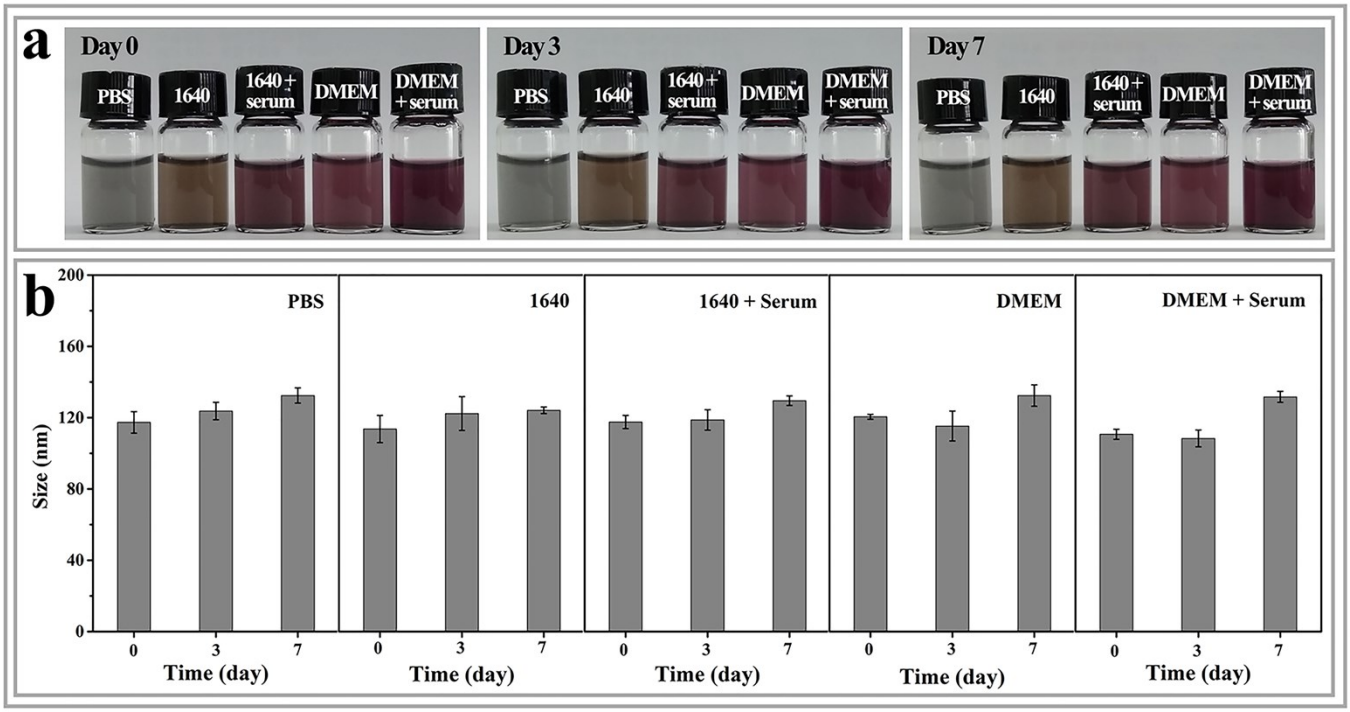

Fig. S5 Time-dependent photographs (a) and hydrodynamic size (b) of WO_{3-x}@HA in PBS, 1640, 1640 + serum, DMEM, DMEM + serum on the 0, 3, and 7 days respectively.

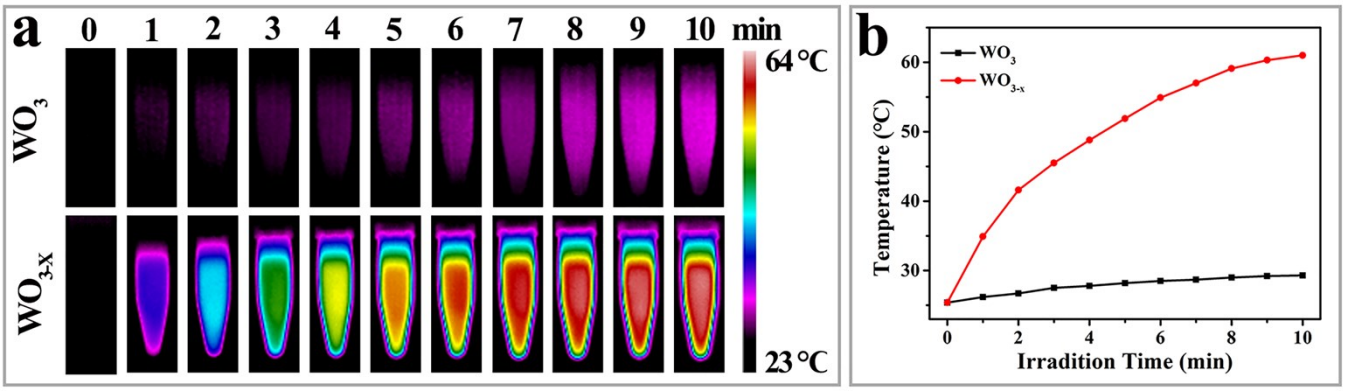

Fig. S6 Photothermal images (a) and heating curves (b) of WO_3 and WO_{3-x} (150 μg/mL) were irradiated with 1064 nm laser (1.0 W/cm^2) for different time.

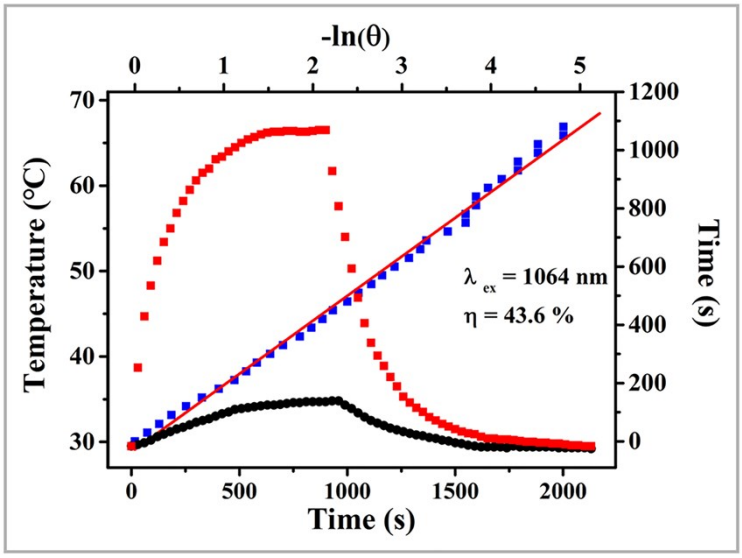

Fig. S7 Photothermal conversion efficiency under irradiation with 1064 nm laser and time constant (τs) for the heat transfer from the system determined by applying the linear time data from the cooling period.

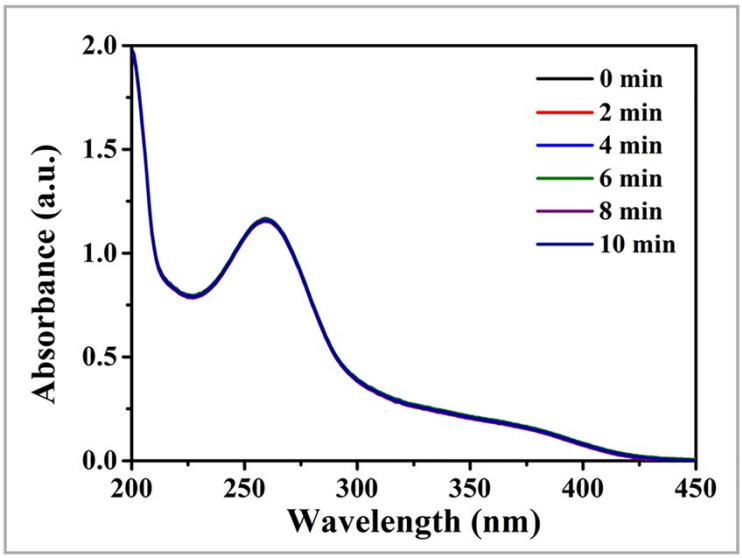

Fig. S8 UV-vis spectrum changes of NBT under 1064 nm laser (1.0 W/cm^2) irradiation.

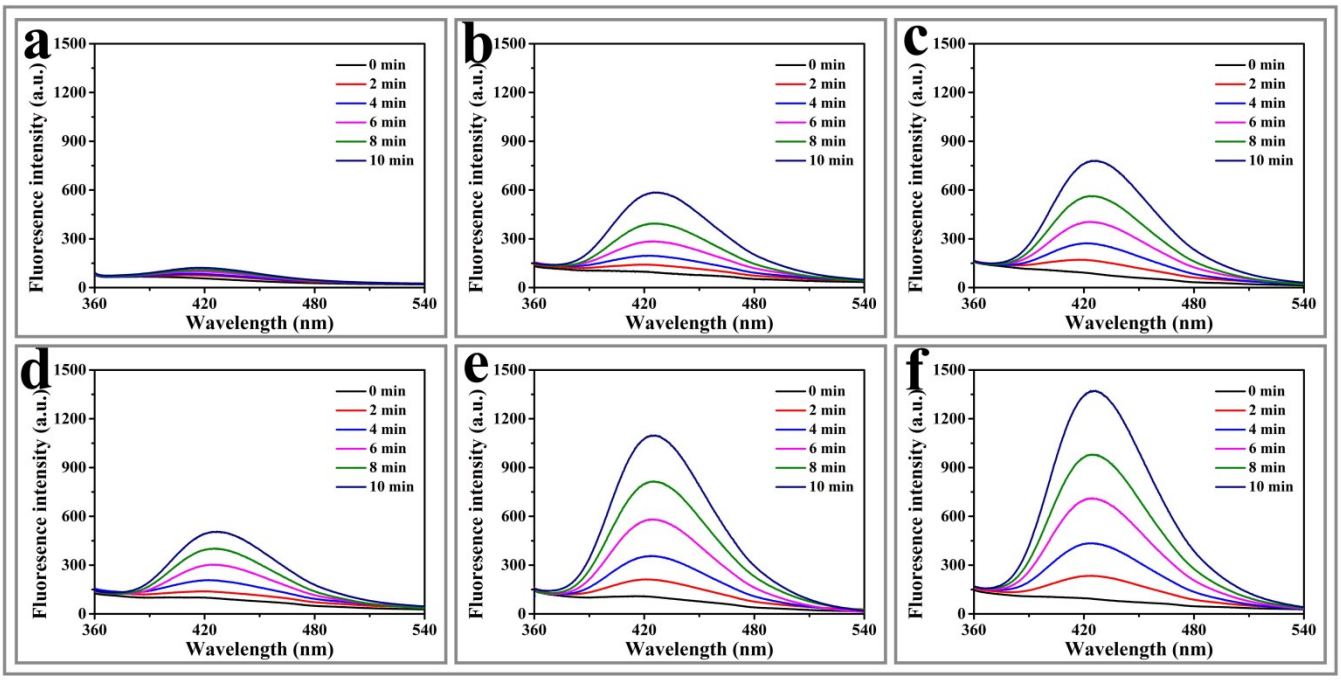

Fig. S9 Fluorescence spectrum of (a) TA 50 °C (b)TA + WO_{3-x}@HA + H_2O_2, (C) TA + WO_{3-x}@HA + H_2O_2 50 °C, (d) TA + WO_{3-x}@HA laser, (e) TA + WO_{3-x}@HA + H_2O_2 + laser 0 °C, (f) TA + WO_{3-x}@HA + H_2O_2 + laser. WO_{3-x}@HA (250 μg/mL), H_2O_2 (100 μM).

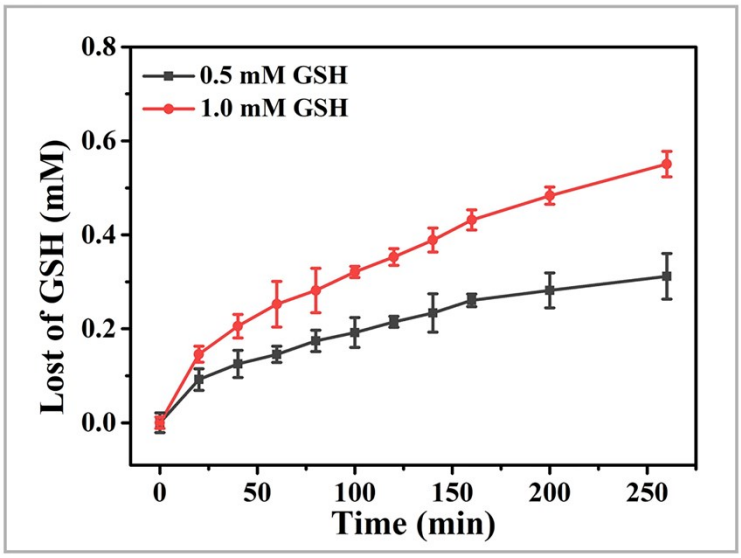

Fig. S10 The lost curves of GSH incubated with WO_{3-x}@HA (250 μg/mL) at variable concentration of GSH.

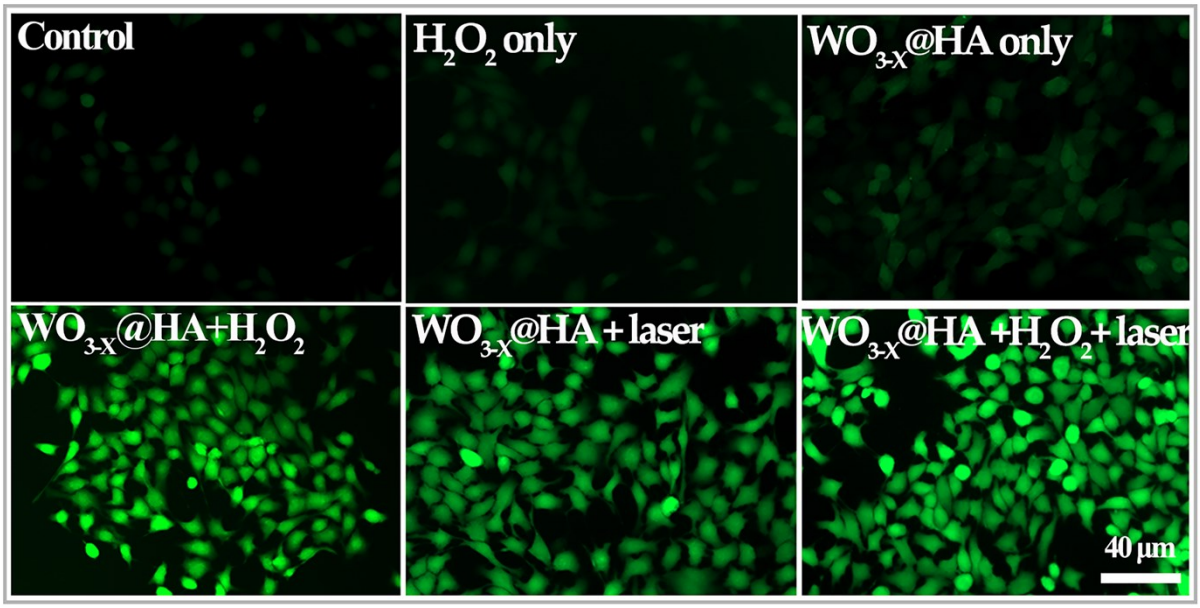

Fig. S11 Fluorescence images of ROS generation in received different treatments for 4T1 cells with WO_{3-x}@HA.

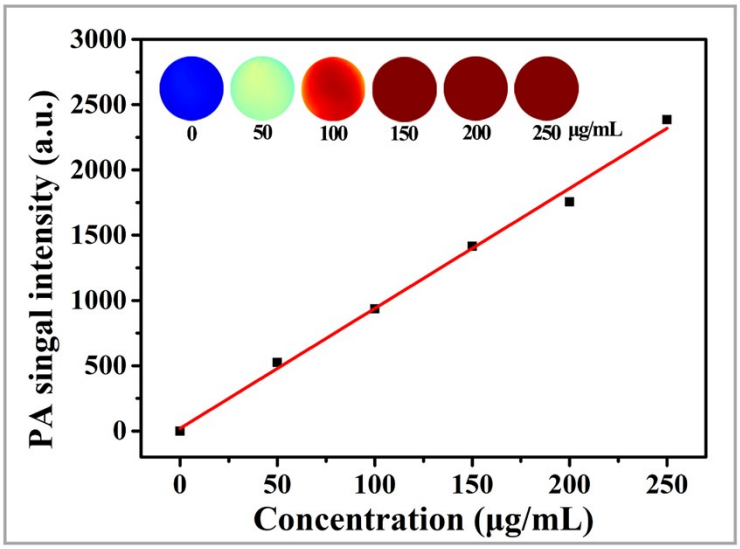

Fig. S12 Linear fitting of PA signal intensity and images of various concentrations of WO_{3-x}@HA.

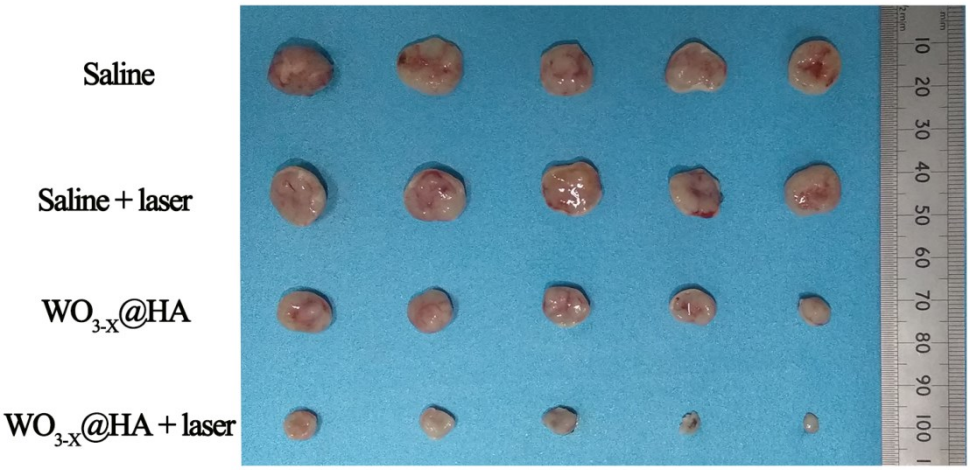

Fig. S13 Photographs of tumour tissues peeled off after the treatment.

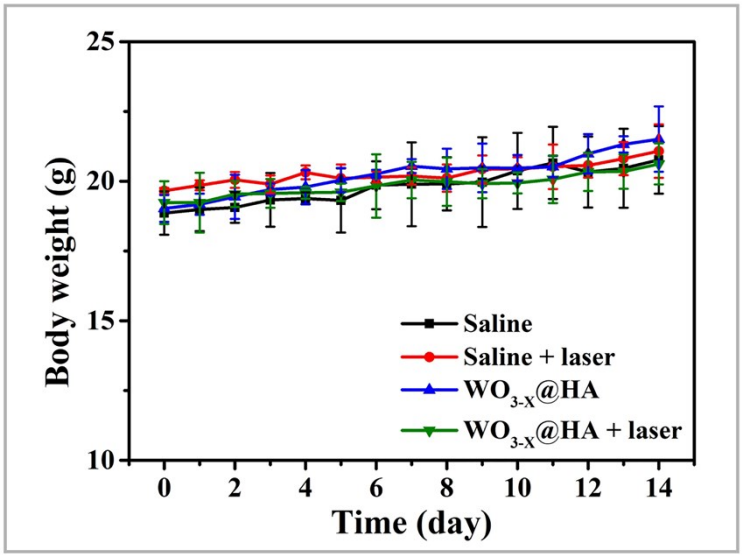

Fig. S14 Weight fluctuation of mice in 14 days post treatments.

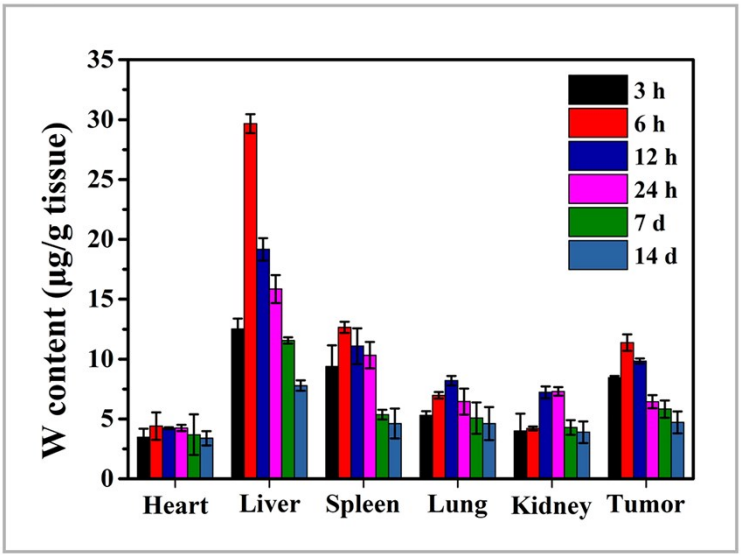

Fig. S15 Biodistribution of W in main organs and tumour tissues of 4T1 tumour-bearing mice after intravenous administration of WO_{3-x}@HA at different time points.

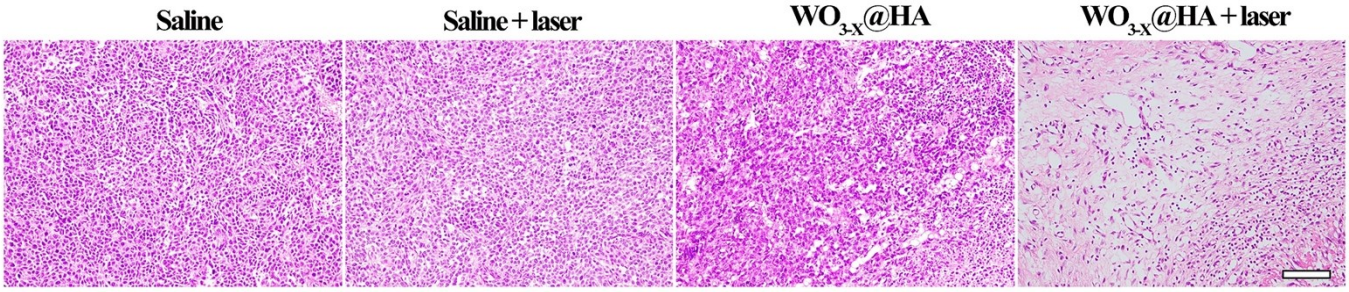

Fig. S16 H&E stained sections of tumour tissues of different groups after different treatment of 14 days. Scale bar: 100 μm.

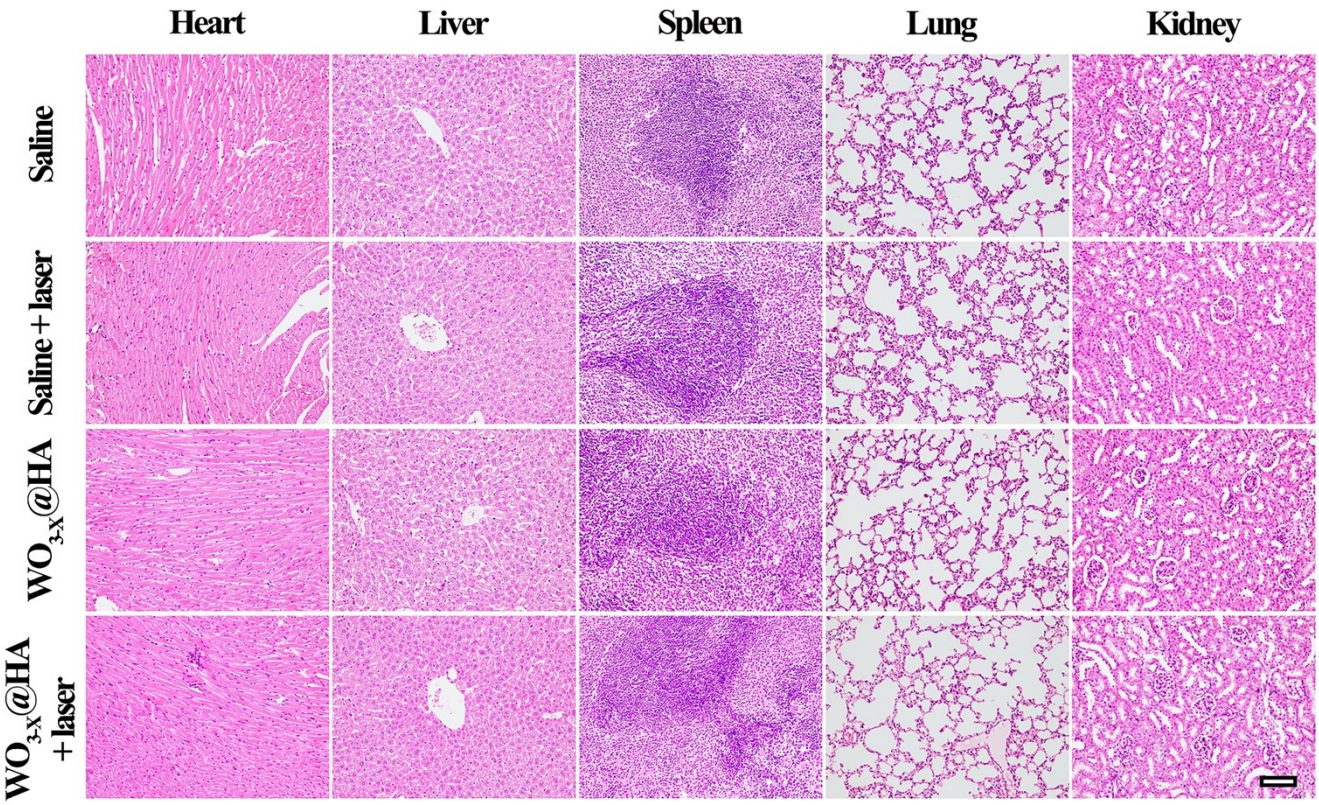

Fig. S17 H&E stained sections of the major tissues after different treatment of 14 days. Scale bar: 100 μm.